

Impact of compatible solutes on the local water structure and the structural organization of lipid monolayers: A combined numerical and experimental study

Jens Smiatek^{1,*}, Rakesh Kumar Harishchandra^{2,†}, Oliver Rubner^{1,‡}, Hans-Joachim Galla^{2,§} and Andreas Heuer^{1,¶}

¹*Institut für Physikalische Chemie, Westfälische Wilhelms-Universität Münster, 48149 Münster, Germany*

²*Institut für Biochemie, Westfälische Wilhelms-Universität Münster, 48149 Münster, Germany*

(Dated: November 13, 2019)

We have performed Molecular Dynamics simulations of ectoine, hydroxyectoine and urea in explicit solvent. Special attention has been spent on the characteristics of the local ordering of water molecules around these compatible solutes. Our results indicate that ectoine and hydroxyectoine are able to bind more water molecules than urea on short scales. Furthermore we investigated the number and appearance of hydrogen bonds between the molecules and the solvent. The simulations show that some specific groups in the compatible solutes are able to form a pronounced ordering of the local water structure. Additionally, we have validated that the charging of the molecules is of main importance. Furthermore we show the impact of a locally varying salt concentration. Experimental results are shown which indicate a direct influence of compatible solutes on the liquid expanded-liquid condensed phase transition in DPPC monolayers. We are able to identify a variation of the local water pressure around the compatible solutes by numerical calculations as a possible reason for an experimentally observed broadening of the phase transition.

INTRODUCTION

Extremolytes are natural compounds which are synthesized by extremophilic microorganisms. Chemically they are organic osmolytes which are build of amino acids, betain, sugar and heteroside derivatives [1]. Thus the name extremolyte is a coinage: organic osmolytes which are synthesized by extremophilic microorganisms. Interestingly, these solutes are biologically inert and accumulate at high concentration in the cytoplasm without interfering with the overall cellular functions; hence they are called *compatible solutes* [2].

The function of these molecules allow microorganisms to resist extreme living conditions like drastic temperature variations and high salinity [1, 3]. A variety of microbiological survival strategies is based on the appearance of extremolytes. For example, high salinity leads to osmolysis, which is only resistable by a cell-inherent water binding mechanism to avoid drying-out. Extremolytes offer an evolutionary answer to the osmolytic stresses the microorganisms are exerted on. Thus the presence of these small molecules is generally focused on the protection of the whole cell.

Long-known compatible solutes in this context are ectoine and hydroxyectoine occurring in anaerobic chemoheterotrophic and halophilic/halotolerant bacteria [2, 4–6]. The structural formulae of these molecules as natural prototypes becomes of interest in this context (Fig. 1). It is obvious that the only difference between ectoine and hydroxyectoine is an additional -OH group.

By experimental investigations, the zwitterionic form of ectoine and hydroxyectoine has been recognized as the stable form in aqueous solution [7, 8] which was later also supported by ab-initio molecular orbital studies [9]. Over the last years the stupendous characteristics of these

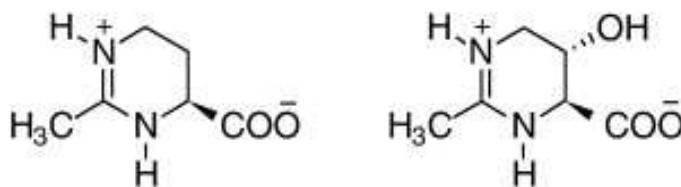


FIG. 1: Structural formulae of ectoine (left) and hydroxyectoine (right).

small molecules have succeeded to explore a novel application area in dermatological industry. Long used hygroscopic molecules like urea have been systematically replaced by extremolytes in a stepwise manner [10]. Specifically ectoine and hydroxyectoine have been used as cell protectants in skin care [3, 10] due to their accessibility of large scale production [1, 4–6].

Experimental investigations on ectoine have further shown additional important biological functions like the stabilization of proteins and cell structure [11, 12]. The reason for this specific protective behaviour can be explained in terms of the preferential exclusion model [13–15]. Within this model it is concluded, that the extremolytes are expelled from the proteins surface as strong water structure formers in a low-water environment such that the growth of the exclusion corresponds to the growth of the excess chemical potential of the protein. This leads to an increase of the solvent accessible surface area and therefore to a preferential hydration of the protein. Once hydrated, the compact native form is conserved and unfolding becomes less favourable.

Molecular Dynamics simulations have indicated [16, 17], that the preferential exclusion model is partly relevant for a specific class of proteins. Additionally it has been

found that the extremolytes do not interact directly with the protein surface but slow down the diffusion of solvent molecules in the bulk phase [16]. The authors conclude that this deceleration is responsible for the restriction of the structural alteration and thereby the enhancement of the kinetic stability.

In addition, Yu *et. al.* [17] reported that some molecules like Chymotrypsin inhibitor II remain for a longer time in presence of ectoine in their native conformation than other proteins *e. g.* Met-Enkephalin. It is concluded that the reason for the particular failure of the model for small proteins like Met-Enkephalin is a lack of a well-defined compact hydration layer which stabilizes the native structure [17]. This leads to a less significant impact of the present compatible solute on the hydration sphere. Nevertheless as the results indicate, the preferential exclusion model is valid for a large variety of proteins with well-defined hydration spheres [17].

Further experiments have shown [13, 18, 19] that extremolytes like ectoine, amino acids and sugars increase the melting temperature of specific proteins. This also can be related back to an enhanced thermodynamic stability of the protein due to the presence of extremolytes and their effects on the hydration sphere.

Even in the context of monolayer structure formation, the presence of extremolytes influence the mechanical properties drastically as experimental results have shown [20]. The results indicate that the compatible solutes lead to a fluidization of monolayers resulting in a more elastic behaviour. The higher fluidity of lipids is advantageous especially for cell membranes for signaling processes. Also repair mechanisms can be accelerated [21]. To summarize, the presence of compatible solutes allows the proteins as well as the cell membranes to resist environmental stresses and to support the regeneration of the native structures.

In this paper we focus on the effects and the characteristics of the hygroscopic behaviour of compatible solutes like ectoine and hydroxyectoine in comparison to urea. We performed Molecular Dynamics simulations in which we investigated the specific influence of extremolytes on the molecular structure of water via radial distribution functions, the solvent accessible surface area and the number of hydrogen bonds. Additionally we calculated the free solvation energy for the compatible solutes which allows to define a quantitative value for hygroscopicity. A further important question is the influence of a varying local salt concentration which is investigated in detail. The results of experiments concerning the relative influence of compatible solutes on lipid monolayer structure formation are presented. It will be shown that the presence of extremolytes supports the mechanical flexibility of lipid monolayers. By the calculation of the local pressure around the solutes, we can elucidate a possible physical description behind this mechanism.

The paper is organized as follows. In the next section we

present the theoretical background. The third section is devoted to the details of the simulations and the experimental techniques whereas the fourth section presents the results. We conclude with a brief summary.

THEORETICAL BACKGROUND

The structure of liquids can be investigated in terms of the radial distribution function [22]

$$g_{AB}(r) = \frac{1}{\langle \rho_B \rangle_l N_A} \sum_{i \in A} \sum_{j \in B}^{N_B} \frac{\delta(r_{ij} - r)}{4\pi r^2} \quad (1)$$

where $\langle \rho_B(r) \rangle$ denotes the particle density of type B at a distance r around particle A and $\langle \rho_B \rangle_l$, respectively $\langle \rho_A \rangle_l$ describes the average particle density of spheres with maximum distance r_{max} with B around A and vice versa. The integral over the distance of Eqn. (1) gives the cumulative radial distribution function which can be transformed into a cumulative particle number function

$$f_{AB}(r) = 4\pi\rho \int_0^r r^2 dr g_{AB}(r). \quad (2)$$

by multiplying Eqn. (1) with the factor $4\pi r^2 \rho$ where ρ is the density of species B or *e. g.* of the solvent.

Specifically in a water environment electrostatic interactions of hydrogen bonds are important for the characteristics of hygroscopicity. If the cumulative particle number function of a molecule with partial charges is compared to an identical molecule without partial charges, the excess number of water molecules indicates an effective hydration value and can be calculated at any distance R . According to the Kirkwood-Buff theory [17, 23], the variation of the solvent can be expressed by the exclusion parameter ν_{cuc} . It is defined by

$$\nu_{cuc}(R) = N_c(R) - \frac{\rho_c(\infty)}{\rho_{uc}(\infty)} N_{uc}(R) \quad (3)$$

where $N_c(R)$ denotes the excess number of solvent molecules around the compatible solutes at a distance R , $N_{uc}(R)$ is the excess number of solvent molecules around the fictive compatible solutes without partial charges at the same distance and $\rho_c(\infty)$ and $\rho_{uc}(\infty)$ are the corresponding solvent densities in the bulk phase. The relative deviations and the ordering of the water can be expressed by the following quantity

$$\xi = 1 + \frac{\nu_{cuc}(R)}{N_{uc}(R)} \quad (4)$$

where $\xi > 1$ represents a hydrophilic and hygroscopic molecule and $\xi < 1$ describes a hydrophobic molecule. A further important quantity is the number of hydrogen

bonds n_{HB} of the compatible solute with the solvent. Taking this number and divide it by the total solvent accessible surface area σ_t at any time gives

$$\rho_{HB} = \left\langle \frac{n_{HB}(t)}{\sigma_t(t)} \right\rangle \quad (5)$$

which is named the hydrogen bond density [17]. It should be noted that the hydrogen bond density is the average number of hydrogen bonds per unit area and not per volume.

Another quantity for the investigation of the hydration ability is the solvation free energy $\Delta F_{\alpha, \text{solv}}$ of species α . A general way to calculate free energy differences in computer simulations is thermodynamic integration [24]. Consider a canonical system in equilibrium where the partition integral can be written to

$$Z_N(N, V, T) = \left(\frac{V^N}{\Lambda_T^N N!} \right) \int d\vec{r}^N e^{-\beta \mathcal{H}(\vec{r}^N)} \quad (6)$$

with the thermal wavelength Λ_T , the inverse thermal energy $\beta = 1/k_B T$ and the Hamilton function $\mathcal{H}(\vec{r})$ for N atoms at positions \vec{r} [24], which defines the free energy to

$$F(N, V, T) = -\frac{1}{\beta} \log Z_N(N, V, T). \quad (7)$$

Free energy differences can then be calculated by the coupling of the Hamiltonian to a perturbation parameter λ which corresponds to a well-defined state [25]. This parameter regulates the strength of the conservative interactions from fully developed to totally vanishing. Thus, the free energy difference between state A and state B is defined by

$$\begin{aligned} \Delta F_{AB} &= F(A) - F(B) = \int_{\lambda_A}^{\lambda_B} \frac{\partial F(\lambda)}{\partial \lambda} d\lambda \\ &= \int_{\lambda_A}^{\lambda_B} \left\langle \frac{\partial \mathcal{H}(\lambda)}{\partial \lambda} \right\rangle d\lambda \end{aligned} \quad (8)$$

where λ is in the parameter range from 0 to 1. This

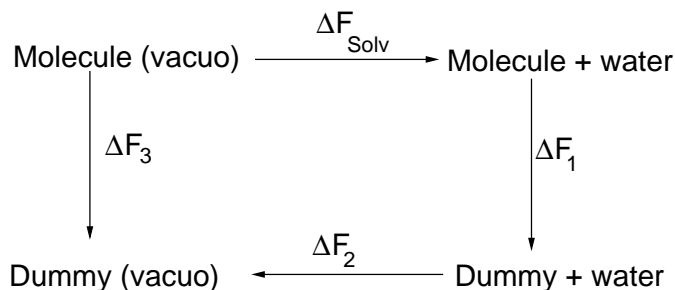


FIG. 2: Thermodynamic cycle for the calculation of solvation free energy differences.

fact can now be used to calculate free solvation energies

[25–27] where $\lambda = 0$ represents the dummy state without interactions in any environment. The corresponding thermodynamic cycle is shown in Fig. 2. The solvation free energy is then defined by

$$\Delta F_{\text{solv}} = \Delta F_3 - \Delta F_1 \quad (9)$$

where ΔF_2 is given by $\Delta F_2 = 0$ due to non-existing interactions. Thus the solvation free energy is associated to the total reversible work that has to be performed to bring the molecule out of a water solution into the vacuum state. Hence the free solvation energy is an accurate estimate for the magnitude and the number of solvent-molecule interactions.

NUMERICAL DETAILS

We have performed Molecular Dynamics simulations in explicit SPC/E water model solvent [28] with the software package GROMACS [29–31] and variations of the force field GROMOS96 [32]. As a starting structure we created the chemical structure via the SMILES language [33, 34]. The topology file with the essential molecular dynamics parameters have been created by the PRODRG server [35]. The structure and the charges of the compatible solutes ectoine and hydroxyectoine and urea have been refined and calculated by the software package TURBOMOLE 6.1 [36]. First we compared the zwitterionic forms to the neutral forms of the compatible solutes. By usage of Møller-Plesset perturbation theory (RI-MP2) and the TZVPP basis set [37, 38], we performed a geometry optimization for the molecules with the COSMO solvent model [39, 40]. We found that the zwitterionic forms of ectoine and hydroxyectoine are 10.81 kcal/mol and 12.35 kcal/mol, respectively, more stable than the neutral counterparts. Thus we chose to neglect the neutral forms for our molecular dynamics simulations.

The corresponding geometry as well as the partial charges for both compatible solutes are presented in Figs. 3 and 4. Having obtained the final structures, we changed the values for the equilibrium parameters, *e. g.* the bond length, partial charges and bond angles in the GROMOS96 force field [32], respectively the PRODRG topology file to the ab-initio results. The same procedure was also done for urea. The missing parameters can be found in the supplementary material.

The molecular dynamics calculations with these structures have been carried out in a cubic simulation box with periodic boundary conditions. The box for the ectoine simulations consisted of $(4.5342 \times 4.5342 \times 4.5342)$ nm filled with 3077 SPC/E water molecules. Hydroxyectoine has been simulated in a box with $(4.6153 \times 4.6153 \times 4.6153)$ nm and 3261 water molecules. The results for urea have been derived in a box of $(4.4015 \times 4.4015 \times 4.4015)$ nm with additional 2803 water molecules. To investigate the influence of the partial charges on the

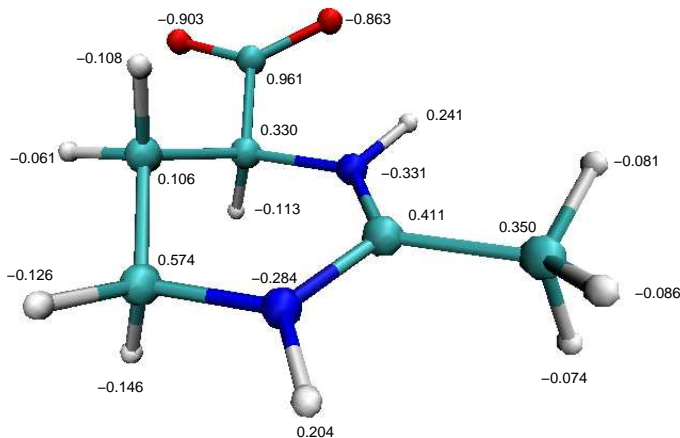


FIG. 3: Lowest energy structure of zwitterionic ectoine with partial charges.

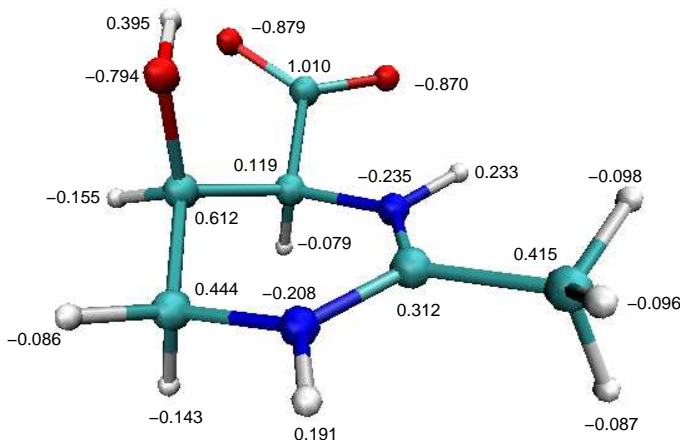


FIG. 4: Lowest energy structure of zwitterionic hydroxyectoine with partial charges.

solvent ordering, we performed simulations where all charges of the compatible solutes have been set to zero. These fictive molecules will be called uncharged in the following.

Electrostatic interactions have been calculated by the Particle Mesh Ewald sum [41] where the whole system was electroneutral. Varying salt concentrations have been achieved by replacing water molecules by the analogue number of chloride and sodium ions.

The timestep was $\delta t = 2$ fs and the temperature was kept constant at 300 K by a Nose-Hoover thermostat [24]. All bonds have been constrained by the LINCS algorithm [42]. After minimizing the energy, we performed 100 ps of equilibration followed by a 10 ns simulation sampling run.

Free energy calculations for the free energies ΔF_1 and ΔF_3 as shown as in Fig. 2 have been performed in independent simulation runs for parameter values of $\lambda \in \{0, 0.1, 0.2, 0.3, 0.35, 0.4, 0.45, 0.5, 0.55, 0.6, 0.65, 0.7, 0.75,$

$0.8, 0.85, 0.9, 0.95, 1\}$. We equilibrated each configuration for 100 ps and the computation of free energy values has been achieved in a 900 ps simulation run for each λ . Due to the appearance of singularities in the conservative interactions for parameter values close to $\lambda = 0$ and $\lambda = 1$, the ordinary potentials have been replaced by the following soft core interaction

$$V_{sc} = (1 - \lambda)V^A \left[(\alpha\sigma^6\lambda + r^6)^{\frac{1}{6}} \right] + \lambda V^B \left[(\alpha\sigma^6(1 - \lambda) + r^6)^{\frac{1}{6}} \right] \quad (10)$$

where $V(r)$ denotes the ordinary electrostatic or van-der-Waals potential in the GROMOS force field in the A-state ($\lambda = 0$) and in the B-state ($\lambda = 1$) [43]. The parameter α has been chosen to 0.7 and the radius of interaction value σ was 0.3.

EXPERIMENTAL DETAILS

The lipids DPPC, (1,2-dipalmitoyl-sn-glycero-3-phosphocholine), used in this study was purchased from Avanti Polar Lipids Inc. (Alabaster, AL). 2-(4,4-Difluoro-5-methyl-4-bora-3a,4a-diaza-s-indacene-3-dodecanoyl)-1-hexadecanoyl-sn-glycero-3-phosphocholine (β -BODIPY[®] 500/510 C₁₂-HPC, BODIPY-PC) was obtained from Molecular Probes (Eugene, OR). The DPPC was dissolved in chloroform/methanol solution (1:1, v/v). Chloroform and methanol were high pressure liquid chromatography grade and purchased from Sigma-Aldrich (Steinheim, Germany) and Merck (Darmstadt, Germany), respectively. Urea was purchased from Roth Chemie GmbH (Karlsruhe, Germany). Ectoine ((S)-2-methyl-1,4,5,6-tetrahydropyrimidine-4-carboxylic acid) and hydroxyectoine ((4S,5S)-2-methyl-5-hydroxy-1,4,5,6-tetrahydropyrimidine-4-carboxylic acid) were obtained from Bitop AG (Witten, Germany). Water was purified and deionized by a multicartridge system (MilliPore, Billerica, MA) and had a resistivity > 18 M Ω m.

Surface pressure-area isotherms were performed on an analytical Wilhelmy film balance (Riegler and Kirstein, Mainz, Germany) with an operational area of 144 cm². All measurements were performed on the subphase containing pure water, ectoine, hydroxyectoine or urea, at 20° C. The DPPC solution was spread on the subphase and left of 10 – 15 min for the solvent to evaporate followed by compressing the monolayer at a rate of 2.9 cm²/min.

Domain structures of DPPC doped with 0.5 mol% BODIPY-PC were visualized by means of video-enhanced epi-fluorescence microscope (Olympus STM5-MJS, Olympus, Hamburg, Germany) equipped with a xy-stage and connected to a CCD camera (Hamamatsu, Herrsching, Germany). The images were captured by

stopping the barrier and equilibrating the monolayer for few minutes at desired surface pressures.

RESULTS

Effects of compatible solutes on the structural organization of monolayers

As we have mentioned in the introduction an important impact of extremolytes on biomolecular assemblies is to sustain the fluidity of membranes under specific circumstances [20]. The mechanical elasticity and flexibility resulting from that effect is important for cell membranes to perform signal processing. Regions with better flexibility are in the liquid expanded LE phase whereas more rigid domains are in the liquid condensed LC phase. The formation of the liquid condensed phase by increasing the surface pressure out of the liquid expanded phase can be described by a phase transition.

Under certain temperature conditions, several domains can be experimentally observed in a lipid monolayer [44, 45]. A driving force to understand the formation of these domains is line tension [46, 47]. Fluid phase coexistence in lipid membranes is characterized by the formation of both liquid condensed phase as well as the liquid expanded phase. The LC phase exhibits a higher degree of ordering and packing preventing water to penetrate the hydrophobic core. Hence the mechanical elasticity is increased in the LE phase. As it has been shown [20] the presence of hydroxyectoine and ectoine alter the formation of the LC domains and therefore ensure the fluidization of the monolayer. This can be described by a variation of the preferential exclusion model [13–17]. A lipid monolayer in water is stabilized by hydrophobic interactions of the apolar lipid tail and hydrophilic interactions of the polar lipid head groups to water. In an ectoine solution the hydrophilic interactions of the monolayer with the solvent are increased by the well coordinated ectoine water complex which results in an increase of the mobility of lipids and hence an increased elasticity of the lipid monolayer [20].

To investigate the above explained effect, we have carried out experiments for monolayers in presence of the different compatible solutes. Therefore we have to compare the results for urea, ectoine and hydroxyectoine on their ability to suppress liquid condensed domain formation. The fluorescence pictures of the monolayers doped with BODIPY-PC, a fluorescent dye that is preferentially soluble in the fluid LE phase are shown in Fig. 5. Dark domains represent the rigidified LC phase, light areas the more fluid LE phase. Lipid films on pure water exhibit the well known kidney shaped LC domains in the phase transition region [20]. The extent of the LC phase increases with increasing surface pressure (decreasing area). The characteristic multi-lobed structure

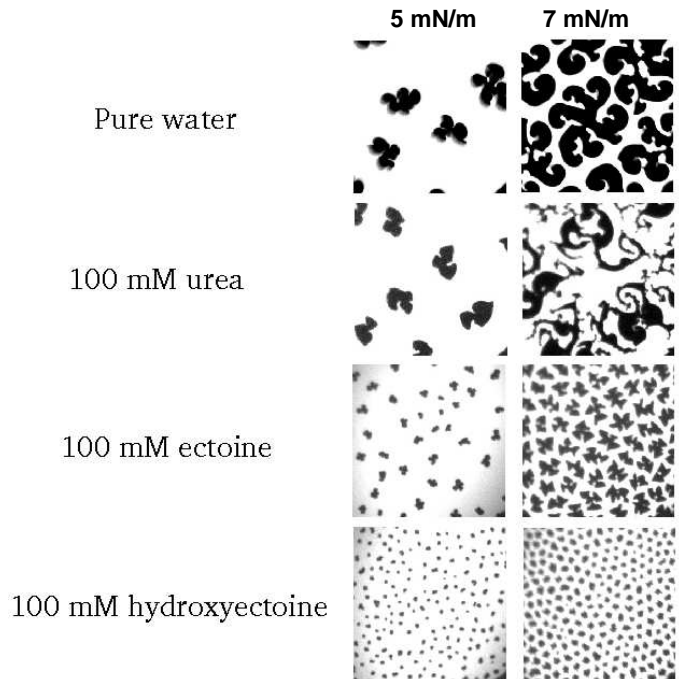


FIG. 5: Video-enhanced fluorescence microscopic images of DPPC monolayers on subphases containing ectoine, hydroxyectoine and urea. All measurements were performed at 20° C and surface pressures 5 (left) and 7 mN/m (right).

starts to form at 5 mN/m and is fully pronounced at 7 mN/m as a left handed clearly developed nanostructure. The presence of urea is only important at 7 mN/m where the domain size compared to pure water is decreased. No visible effect can be observed at 5 mN/m. Ectoine at 5 mN/m leads to a considerable shrinkage in the domain size. At 5 mN/m and 7 mN/m the well developed domain structure is therefore lost continuously. This effect is even more enhanced on a subphase containing hydroxyectoine.

To investigate this effect in more detail, we have studied the local surface pressure π experimentally. The results for the surface pressure-area isotherms are shown in Fig. 6. The isotherm of DPPC on pure water shows a phase transition from the LE- to the LC regime at 5 mN/m by an almost constant pressure during compression of the film between areas of 7.8-5 nm². Additionally urea also shows this phase transition at roughly 5 mN/m from 8 to 5.5 nm². Indeed, isotherms taken on ectoine and hydroxyectoine containing subspaces are shifted to higher area values and the LE to LC phase transition is broadened. At high pressures ($\pi > 25$ mN/m) the isotherms merge thus clearly showing that the compatible solutes do not influence the lipid structural organization. However it can be seen, that the effect for hydroxyectoine is more pronounced compared to ectoine and urea. As a driving force for the decrease of the rigidity of the lipids

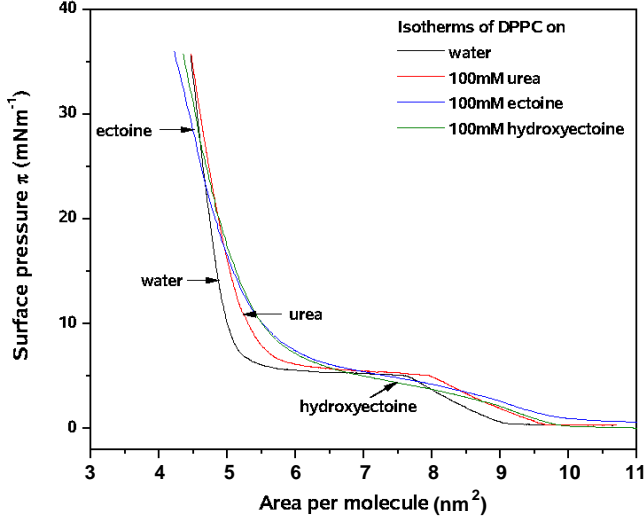


FIG. 6: Surface pressure isotherms for DPPC in presence of the different compatible solutes in comparison to the solvent accessible area of a DPPC molecule

in presence of the compatible solutes, we propose a direct influence of the local water pressure exerted on the monolayer.

Therefore we have calculated numerically by Molecular Dynamics simulations the local pressure around the compatible solutes in the water bulk phase by the method proposed in [48]. For this we fixed the compatible solutes in the center of the simulation box assuming a spherical symmetry. The water molecules have been kept mobile. The importance of a local water pressure variation and its influence on the properties of the monolayer can be seen by

$$\pi(z) = P_L(z) - P_N(z) \quad (11)$$

where π denotes the lateral pressure profile, P_L the lateral pressure component and P_N the normal component of the pressure tensor, which can be related to the bulk solvent pressure [49, 50]. Hence a decrease in the bulk pressure is related to an increase of the lateral pressure profile. The results for the local pressure in the bulk solvent phase are displayed in Fig. 7. If we assume a constant area for the monolayer, the above explained behaviour due to a decrease of the bulk solvent pressure can be observed. Thus a broadening of the phase transition can be explained by a decrease of the normal pressure component related to the presence of compatible solutes on small length scales. Hence it can be concluded, that compatible solutes which are able to decrease the local solvent pressure indirectly influence the properties of monolayers by increasing the lateral pressure which is mainly related to the mechanical flexibility. Large negative values can be observed for urea on distances up to 0.45 nm. Hydroxyectoine and ectoine have negative val-

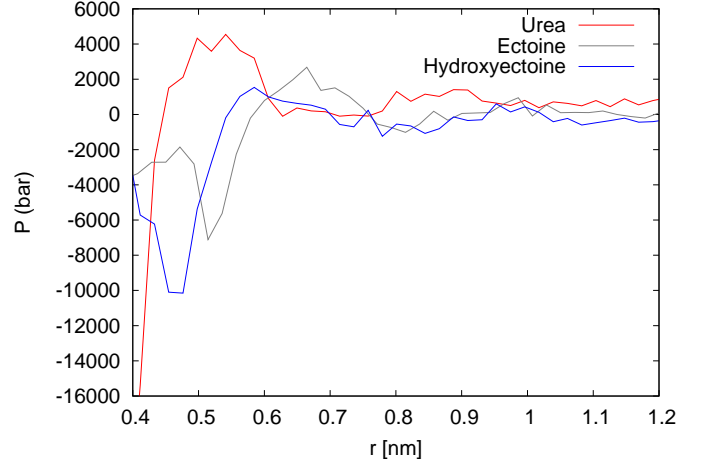


FIG. 7: Pressure in the bulk water phase around the compatible solutes.

ues on distances up to 0.55 and 0.6 nm, respectively. It is obvious that the local pressure on scales 0.45-0.55 nm is drastically decreased in presence of ectoine. Hydroxyectoine additionally has a direct impact on the local pressure by a large reduction on scales 0.425 to 0.525 nm. Hence, water molecules are strongly correlated to the compatible solute on the mentioned lengthscales indicated by the negative values, such that the normal pressure on the monolayer is decreased in the direction of the extremolyte.

Very short distances which are smaller than 0.4 nm indicate a direct interaction like hydrogen bonds with the monolayer. Hence one can conclude, that the local pressure decrease for urea happens on too short length scales ($r < 0.4$ nm) leading to direct uneffective interactions with the monolayer as reported in [17] for extremolytes. Instead on a lengthscale larger than 0.8 nm only statistical noise fluctuating around zero can be observed for all molecules. For the above reasons, we can conclude that the lengthscale $r = 0.4 - 0.6$ nm is the most important one for the influence of the compatible solutes on the lipid monolayer. This is in agreement to [17], where the typical distance between ectoine and the cosolute was identified to be above 0.4 nm. The drastic influence on the local water pressure respectively the monolayer in the important interval $r = 0.4 - 0.6$ nm is also obvious by regarding the average values of the local pressure. Hydroxyectoine has an average pressure of -4215 bar, ectoine a value of -3186 bar and urea a positive value of 547 bar which is in qualitative agreement to the results shown in Figs. 5 and 6 where the effect is even more pronounced for hydroxyectoine in comparison to ectoine in agreement to the experimental results. The presence of urea alters the monolayer structure formation on a lengthscale smaller than 0.45 nm which can be related to direct interactions.

TABLE I: Free solvation energy ΔF_{solv} for the different compatible solutes.

Molecule	ΔF_{solv} [kJ/mol]
Urea	-164.83 ± 2.02
Ectoine	-283.87 ± 3.38
Hydroxyectoine	-318.85 ± 3.72

Structural properties of compatible solutes and their influence on the local water structure

To understand the microscopic origins of the pressure variations, we analyzed the structural properties of ectoine, hydroxyectoine and urea and their influence on the local solvent properties. As it has been mentioned in the introduction, the water-binding ability is one of the key ingredients to suppress drying out by osmolytic. A significant quantity to investigate the potential hygroscopicity is given by the solvation free energy of the compatible solutes. Molecules with large negative free solvation energies can be identified as highly soluble. The free energy difference can therefore be interpreted as the total reversible work associated by changing the environment around the solute from the vacuum state to the liquid state. Hence one can conclude that a large number of direct solvent-solute interactions are responsible for a good solubility.

As the values of Tab. I indicate, drastic deviations can be observed for the different solutes. The molecule with the largest negative free energy of solvation is hydroxyectoine whose value is twice as large as the value for urea. Thus one can guess that ectoine and hydroxyectoine have more pronounced direct interactions with water in contrast to urea.

To investigate the specific nature of these interactions we have calculated the solvent accessible hydrophilic surface area σ_h [51] which is compared to the total solvent accessible surface area to give the ratio r_σ . Additionally we have computed the hydrogen bond density ρ_{HB} defined by Eqn. 5 and the number of hydrogen bonds n_{HB} . A hydrogen bond is defined as existent, if the distance between the interacting atoms is closer than 0.35 nm and the angle is not larger than 30 degrees. Regarding the different number of hydrogen bonds and the free energies given in Tab. I, we identify the free energy per hydrogen bond area $\Theta = \Delta F_{solv}/n_{HB}$ as another quantity of interest. To further estimate the influence of the charged functional groups, we conducted simulations where the partial charges had been set to zero such that the whole compatible solute was uncharged. This value was subtracted from the average number of hydrogen bonds n_{HB} resulting in the net average number of hydrogen bonds n_{HB}^c . The results are displayed in Tab. II. Although

TABLE II: Hydrophilic surface σ_h and its ratio of the total surface r_σ , number of hydrogen bonds n_{HB} , net number of hydrogen bonds n_{HB}^c , average hydrogen bond density ρ_{HB} and average free energy per hydrogen bond Θ .

Molecule	Urea	Ectoine	Hydroxyectoine
σ_h [nm ²]	1.41 ± 0.01	1.63 ± 0.01	1.73 ± 0.01
r_σ	1	0.64 ± 0.01	0.67 ± 0.01
n_{HB}	4.43	7.01	8.77
n_{HB}^c	3.35	6.31	7.75
ρ_{HB} [nm ⁻²]	3.08 ± 0.03	2.77 ± 0.01	3.42 ± 0.02
Θ [kJ/mol]	-49.20	-44.99	-41.20

the whole solvent accessible surface area of urea is hydrophilic, this seems not to be the reason for the large free energies if the values for all molecules are compared to the data values displayed in Tab. I. Thus one can conclude that the amount of a hydrophilic surface for small molecules is more important than the ratio. This becomes even clearer by regarding the large values for the hydrogen bond density. Hence, it is obvious that the main contribution to the solvation free energy is given by direct spatial interactions like hydrogen bonds. This becomes obvious by regarding the average and net average values for the hydrogen bonds. Ectoine and hydroxyectoine have more than seven and nearly nine hydrogen bonds, respectively, in contrast to urea with four bonds. Even the net average numbers are large indicating the relative importance of the partial charging. Thus these values show that the hydrogen bonds between the solvent and the solute are mainly responsible for the good hygroscopic behaviour of the compatible solutes. This assumption is further validated by the free energy per hydrogen bond Θ which accounts for the direct binding and its relative energy. All values for Θ are comparable indicating the importance of the hydrogen bonds and their influence on the free energy of solvation. Both ingredients can therefore be related to the fact that a high charging resulting in a large number of hydrogen bonds and a relatively small size are related to large exothermic solvation energies [52]. It can be assumed that a molecule whose size is in the same range of water molecules like ions, with many charged groups is more suited to induce a strong effect of water ordering than larger molecules with hydrophobic surfaces like proteins [52]. Regarding the values for Θ which compares the ratio of the free energy to the number of hydrogen bonds it is evident that the number of hydrogen bonds are summed in the value of the free solvation energy. Thus, hydroxyectoine and ectoine are more hygroscopic than urea. Nevertheless, it has to be mentioned that this ranking is induced by

TABLE III: Average hydrogen bonds and average lifetime per functional group (in brackets) per molecule.

Group	Ectoine	Hydroxyectoine	Urea
R1	5.59 (11.99 ps)	5.26 (13.08 ps)	–
R2	0.68 (5.81 ps)	0.84 (7.78 ps)	–
R3	0.75 (6.89 ps)	0.69 (6.32 ps)	–
R4	–	1.98 (9.89 ps)	–
R5	–	–	0.90 (5.24 ps)
R6	–	–	0.83 (5.35 ps)
R7	–	–	2.71 (13.40 ps)

a general high level of hygroscopicity for the molecules compared to other solutes.

We further investigated the importance of the functional

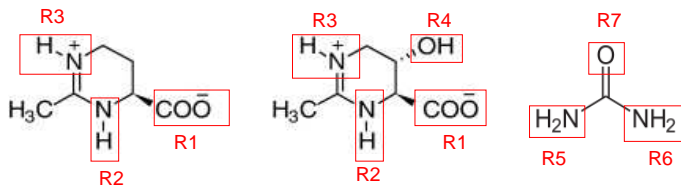


FIG. 8: Schematic highly charged groups in ectoine (left), hydroxyectoine (middle) and urea (right).

groups for the hydrogen bonds. Therefore we identified the most highly charged groups in each molecule and numbered them by the acronyms R1-R7 (Fig. 8). The data together with the corresponding average lifetimes are displayed in Tab. III with the notation given in Fig. 8. We defined a hydrogen bond as existent if the distance between the interacting atoms is closer than 0.35 nm and the angle is not larger than 30 degrees. The largest number of hydrogen bonds appears at the carboxylic group (R1) of the extremolytes. The largest value for urea is induced by the oxygen group (R7). The lifetimes for a hydrogen bond of urea (R7) and for the extremolytes (R1) are comparable. For a comparison, the average lifetime of hydrogen bonds in pure water in our simulations has been found to be around 2.72 ps. Thus one can conclude by comparing the values above to the pure water value that all the bonds displayed in Tab. III are well coordinated and established. A Simulation snapshot of a hydroxyectoine molecule in water is shown in Fig. 9. All water molecules form hydrogen bonds to hydroxyectoine and are located within a distance of 0.35 nm and an angle of 30 degrees. It can be seen that most of the water molecules are interacting with the carboxylic group (R1) in agreement to the results of Tab. III.

The results for the radial distribution function for wa-

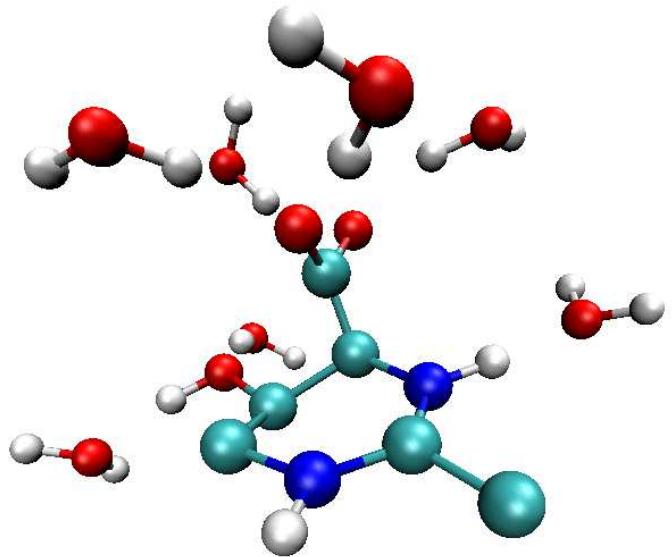


FIG. 9: Simulation snapshot of hydroxyectoine in solution with surrounding water molecules. All water molecules form a hydrogen bond to the hydroxyectoine and are located within a distance of 0.35 nm and an angle of 30 degrees. Shown are the carbon atoms and the polar groups.

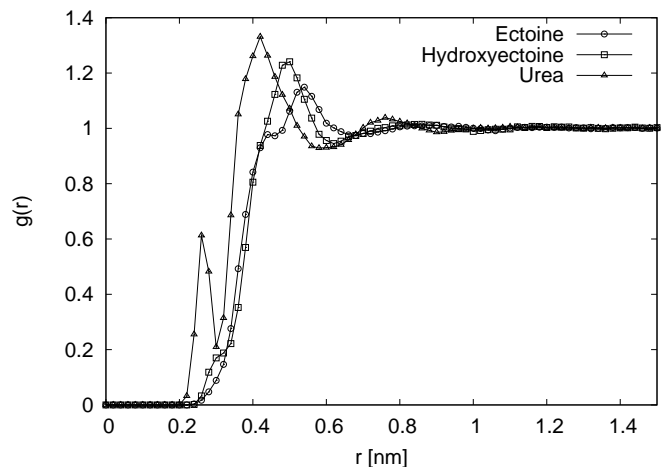


FIG. 10: Radial distribution function $g(r)$ for water molecules around the compatible solutes ectoine, hydroxyectoine and urea.

ter molecules around the compatible solutes are shown in Fig. 10. At a first glance, hydroxyectoine and ectoine have nearly identical distribution functions with pronounced peaks at 0.5 nm (hydroxyectoine) and 0.54 nm (ectoine). Urea shows two pronounced peaks at 0.24 nm and 0.4 nm. This can be explained by the smaller size of urea compared to the other molecules which allows the water molecules to get closer to the center of mass. Nevertheless the influence on the molecular water structure decays around 1 nm to reach the bulk value of pure water for all molecules. Thus the main influence of

the compatible solutes on the water molecules is located within this distance.

A more detailed investigation in dependence of the water structure on the functional groups has also been performed (data not shown). The carboxylic group R1 is able to form a pronounced structuring of the water molecules around distances 0.22 and 0.34 nm. Nevertheless, the main contribution at 0.54 nm for ectoine and 0.5 nm for hydroxyectoine as indicated in Fig. 10 is related to the coordination of all present functional groups. Hence at these distances all highly charged groups are able to bind water molecules which gives a concerted contribution to the radial distribution function resulting in the peaks shown in Fig. 10. The hydroxy group (R4) of hydroxyectoine is even able to form a water peak at 0.22 nm. The large peak for urea at 0.2 nm is related to the oxygen (R7). Thus it can be concluded that oxygen atoms in all molecules are able to form a pronounced layering even at very short distances.

The radial cumulative number distribution function

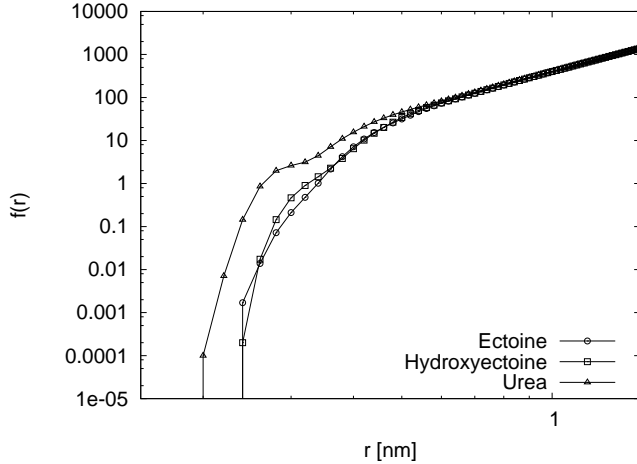


FIG. 11: Radial cumulative number distribution function $f(r)$ for water molecules around all compatible solutes.

is presented in Fig. 11. The pronounced accumulation of water molecules around urea at short scales up to 0.4 nm due to its smaller size is evident. The cumulative number distribution function for ectoine and hydroxyectoine is again nearly identical in agreement to Fig. 10. Nevertheless, the net effect of water accumulation can only be considered by the comparison to a reference system. To realize this system, we conduct simulations with uncharged compatible solutes, meaning neglecting all partial charges. The results for the distribution function created by these simulations are then used to define a reference value with an identical excluded volume to neglect size effects. The results for the difference in the radial cumulative number distribution function $\Delta f(r) = f_c(r) - f_{uc}(r)$ are shown in Fig. 12. It is striking that hydroxyectoine is able to bind up to nine net

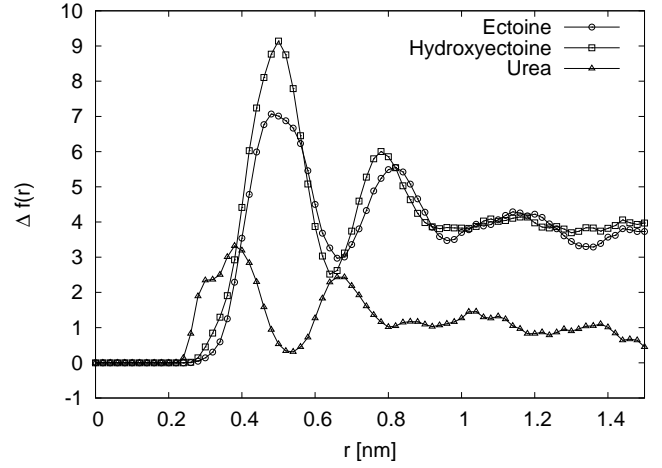


FIG. 12: Difference of the radial cumulative number distribution function $\Delta f(r)$ as defined in the text for water molecules around all compatible solutes.

water molecules, respectively seven water molecules for ectoine up to a distance of 0.5 nm. In contrast to these molecules, urea can bind up to three molecules. These results are again closely related to the average number of hydrogen bonds displayed in Tab. III. Even at distances larger than 1 nm, the net gain is given by four molecules for the extremolytes in contrast to urea which has an effective net gain of one molecule. Thus the indirect long range influence of extremolytes on the local water structure is evident. Hence it can be seen that hydroxyectoine and ectoine are more hygroscopic than urea. Furthermore the larger values for hydroxyectoine in contrast to ectoine are related to the hydroxy group (R4) which is additionally responsible for 1.977 hydrogen bonds (Tab. III).

Regarding Eqn. 4, the relative deviation at any distance

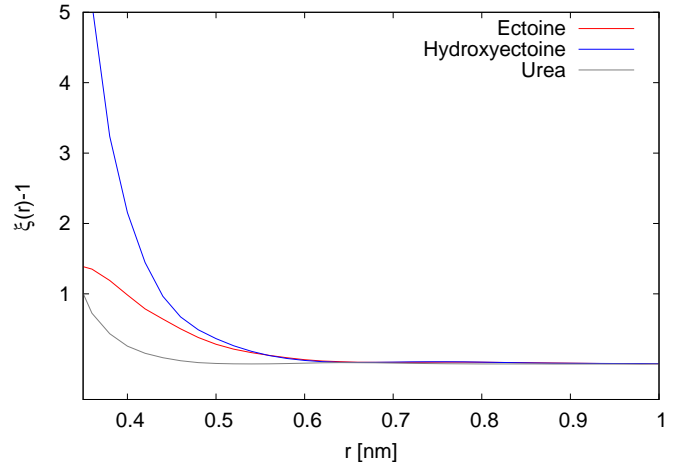


FIG. 13: Relative deviation $\xi - 1$ for all compatible solutes.

between the charged and uncharged cumulative radial

number distribution functions can be expressed by

$$\frac{N_c - N_{uc}}{N_{uc}} = \xi - 1 \quad (12)$$

where the results are shown in Fig. 13. Compared to the above presented results the main perturbation of the water structure around urea decays on lengthscales up to 0.4 nm whereas the values for hydroxyectoine and ectoine decay on larger scales up to 0.6 nm. Again, the larger values for hydroxyectoine compared to ectoine at $r < 0.4$ nm can be related to the additional hydroxy group (R4). However the relative deviations on small scales are in general very large compared to other molecules. This proves the assumption that hydrogen bonds induce a direct impact on the ordering of the local water structure. Furthermore it is evident, that all mentioned length scales are identical to the variations of the local pressure in the last section. Hence the local ordering of the water induced by the large number of hydrogen bonds in addition to the evident water accumulation on small length scales explains the effect of the local pressure decrease around the extremolytes.

Influence of a varying salt concentration

Another interesting quantity is the direct influence of salt on the hygroscopicity of the solutes. As it was mentioned in the introduction, extremolytes are able to resist osmolytic stress of the cell even at high salinity. Therefore we expect the influence of salt on the function of extremolytes to be negligible.

To investigate this point in more detail, we simulated salt solutions whose concentration values are in the range from 0.017 mol/L to 0.107 mol/L which is comparable to experimental and physiological conditions [1]. As it can be concluded from the data shown above, a main reason for a deliquescent behaviour is given by a large number of apparent hydrogen bonds. Thus one can conclude that if the influence of salt achieves a decrease in the number of hydrogen bonds, extremolytes are sensible to the salt concentration which stands in contrast to their biological function. Therefore we have compared the number of hydrogen bonds with increasing salt concentration (Fig. 14) and their time of existence (Fig. 15) given by the ratio to the values of the no-salt simulations shown in Tab. II. As Fig. 14 indicates the ratio is always above 0.97 indicating the neglect of a direct influence of salt on the number of hydrogen bonds. The same behaviour can also be observed in Fig. 15. The results indicate that the existence times are nearly identical or are slightly diminished down to 0.92. Hence we conclude, that an increasing salt concentration does not vary the ability of extremolytes to bind water molecules nor to vary the quality of the bonds. Therefore it can be concluded that

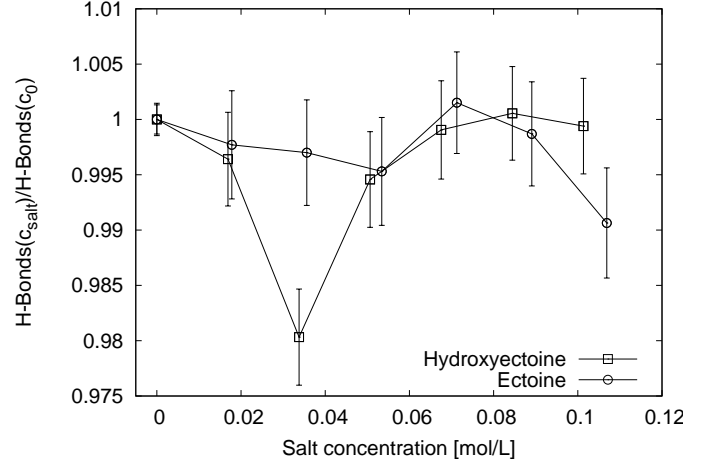


FIG. 14: Number of hydrogen bonds in presence of salt divided by the average values without salt given by Tab. II

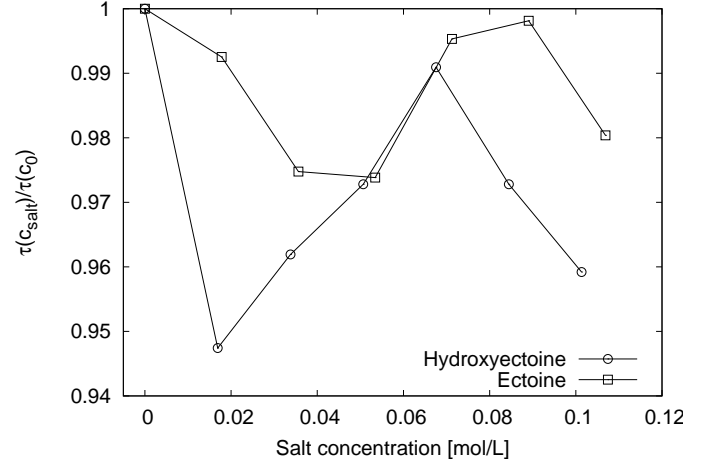


FIG. 15: Average existence time for a hydrogen bond in presence of salt divided by the average values without salt given by Tab. II

high salinity does not affect the biological function due to charge screening effects.

SUMMARY AND CONCLUSION

In this paper we investigated the solvent properties around the compatible solutes ectoine, hydroxyectoine and urea and their influence on the local structure of monolayers. For this we studied experimentally the impact of the compatible solutes on the formation of domains in the LE-LC phase transition for monolayers. Our results indicate that ectoine and hydroxyectoine broaden the phase transition between the LE-LC coexistence isotherme and suppress the appearance of LC do-

mains. Thus the mechanical flexibility of the monolayer is supported by the presence of extremolytes. To investigate the experimental results in more detail, we have numerically calculated the local pressure around the compatible solutes in Molecular Dynamics simulations which is drastically lowered on length scales ranging from 0.4 to 0.6 nm for ectoine and hydroxyectoine in contrast to urea. This decrease of the local pressure results in an increase of the lateral surface pressure of the monolayer which has been observed earlier [20] and is in agreement to the experimental results.

To study the origins of the local pressure variation in detail, we investigated the microscopic deliquescent properties of the compatible solutes and their influence on the local water structure. Our results indicate that ectoine and hydroxyectoine are able to bind more water molecules than urea. Thus the usage of extremolytes as water binding chemical detergents in dermatologic products is validated. By comparison to the uncharged, purely steric interacting species we found that the extremolytes are able to bind up to nine water molecules for hydroxyectoine, respectively seven for ectoine in a distance located within 0.6 nm. Even the long scale water accumulation for distances above 1 nm is evident. The reason for this is the formation of a large number of hydrogen bonds at specific functional groups of the molecules. The most important group for extremolytes to form hydrogen bonds is the charged carboxylic group. Our results indicate a direct local water ordering on distances up to 0.6 nm.

Thus we conclude that the charging of the extremolytes is of main importance. Related to that topic is the large negative free energy of the extremolytes and the relatively large hydrophilic surface area compared to the total solvent accessible surface area. Nevertheless it has to be mentioned, that all investigated compatible solutes are very small molecules. Hence, in accordance to ions, the general assumption of solubility, which states that a large exothermic energy is related to large charge values and small radii can be also applied for the studied extremolytes [52]. Thus, small molecules with large charge values show a distinct hygroscopic behaviour. Although urea is smaller than the other molecules and has a total hydrophilic overall surface, the zwitterionic character of the extremolytes allows to accumulate more net water molecules resulting in a stronger ordering effect. This is also related to the present number of hydrogen bonds with the compatible solutes. It is evident that the extremolytes have a large number of hydrogen bonds in comparison to their small solvent accessible surface. To summarize these points, if a small molecule is charged and mainly hydrophilic it can be seen as hygroscopic if a large number of direct solvent-solute interactions can be identified. This becomes also obvious by regarding the comparable values for all compatible solutes in the free solvation energy per hydrogen bond Θ .

Although the extremolytes are charged and act via electrostatic interactions with the solvent, we have shown that the presence of salt does only slightly alter the quality and the number of hydrogen bonds. Hence, the specific water binding behaviour of the compatible solutes is not lost at high salinity as the biological function of the extremolytes demands.

We have further investigated the influence of the surface properties on the hygroscopic properties. It has been shown that all compatible solutes have a large hydrophilic to total solvent accessible surface area ratio. Compared to their small size, all investigated molecules can form a distinct number of hydrogen bonds. Closely related to this are the calculated solvation free energy values which indicate strong solvent-solute interactions for all compatible solutes. Thus the extremolytes show an extraordinary hygroscopic behaviour due to the following closely related properties. They are zwitterionic, resulting in a high partial charging. Furthermore the extremolytes are small molecules with a mainly hydrophilic surface. These properties result in a large number of hydrogen bonds in a small volume indicating a drastic impact on the local water structure which increases the free solvation energy. Due to the larger number of hydrogen bonds compared to urea, ectoine and hydroxyectoine are more able to show deliquescent properties resulting in the observed pressure decrease around the molecules in the bulk solvent phase. For the above reasons one can therefore identify extremolytes as water-binding molecules which order the local structure of the solvent up to lengthscales of 0.6 nm significantly.

To summarize the effects on the water molecules, we have shown that the largest ordering effect can be related back to the influence of some specific functional groups of the extremolytes. The water molecules are therefore placed around the characteristic functional group and form hydrogen bonds.

The evolutionary strategy to overcome dry situations for microorganisms by the synthesis of extremolytes is supported by our data. All our results indicate that ectoine and hydroxyectoine are better suited for these extreme situations than long known hygroscopic molecules like urea.

Thus the addition of extremolytes in contrast to urea in dermatological products is validated from a physical and chemical point of view.

ACKNOWLEDGEMENTS

Financial support by the Deutsche Forschungsgemeinschaft (DFG) through the transregional collaborative research center TRR 61 is gratefully acknowledged. R. K. Harishchandra acknowledges funding from the International Graduate School in Chemistry at the University of Münster.

-
- * Electronic address: jens.smiattek@uni-muenster.de
 † Electronic address: r'hari01@uni-muenster.de
 ‡ Electronic address: rubner@uni-muenster.de
 § Electronic address: gallah@uni-muenster.de
 ¶ Electronic address: andheuer@uni-muenster.de
- [1] Lentzen G. and Schwarz T., *Appl. Microbiol. Biotechnol.* **72**, 623 (2006)
 - [2] Brown A. D., Rose A. H. and Morris J. G., *Advances in Microbial Physiology* **17**, 181 (1978)
 - [3] Graf R., Anzali S., Buenger J., Pfluecker F. and Driller H., *Clinics in Dermatology* **26**, 326 (2008)
 - [4] Galinski E. A., Pfeiffer H. P. and Truper H. G., *Eur. J. Biochem.* **149**, 135 (1985)
 - [5] Galinski E. A., *Experientia* **49**, 487 (1993)
 - [6] Inbar L. and Lapidot A., *J. Biol. Chem.* **263**, 16014 (1988)
 - [7] Schuh W., Puff H., Galinski E. A. and Truoeer H. G., *Z. Naturforschung* **40c**, 780 (1985)
 - [8] Inbar L., Frolov F. and Lapidot A., *Eur. J. Biochem.* **214**, 897 (1993)
 - [9] Suenobu K., Nagaoka M., Yamabe T. and Nagata S., *J. Phys. Chem. A* **102**, 7505 (1998)
 - [10] Dirschka T., *Akt. Dermatol.* **34**, 115 (2008)
 - [11] Lamosa P., Turner D. L., Ventura R., Maycock C. and Santos H., *Eur. J. Biochem.* **270**, 4604 (2003)
 - [12] Foord R. L. and Leatherbarrow R. J., *Biochemistry* **37**, 2969 (1998)
 - [13] Lee C. J. and Timasheff S. N., *J. Biol. Chem.* **256**, 7193 (1981)
 - [14] Arakawa T. and Timasheff S. N., *Arch. Biochem. Biophys.* **224**, 169 (1983)
 - [15] Arakawa T. and Timasheff S. N., *Biophys. J.* **47**, 411 (1985)
 - [16] Yu I. and Nagaoka M., *Chem. Phys. Lett.* **388**, 316 (2004)
 - [17] Yu I., Jindo Y. and Nagaoka M., *J. Phys. Chem. B* **111**, 10231 (2007)
 - [18] Knapp S., Ladenstein R. and Galinski E. A., *Extremophiles* **3**, 191 (1999)
 - [19] Yancey P. H., Clark M. E., Hand S. C., Bowlus R. D. and Somero G. N., *Science* **217**, 1214 (1982)
 - [20] Harishchandra R. K., Wulff S., Lentzen G. Neuhaus T. and Galla H.-J., *Biophys. Chem.* **150**, 37 (2010)
 - [21] Bünger J., Degwert J. and Driller H., *IFSCC-Magazine* **4**, 2 (2001)
 - [22] Allen M. P. and Tildesley D. J., *Computer simulation of liquids*, Oxford Science Publications, Oxford (1987)
 - [23] Kirkwood J. G. and Buff F. P., *J. Chem. Phys.* **19**, 774 (1951)
 - [24] Frenkel D. and Smit B., *Understanding Molecular Simulation*, Academic Press, San Diego (1996)
 - [25] Kollman P., *Chem. Rev.* **93**, 2395 (1993)
 - [26] Garrido N. M., Jorge M., Queimada A. J., Economou I. G. and Macedo E., *Fluid Phase Equilibria* **289**, 148 (2010)
 - [27] Leach A., *Molecular Modeling: Principles and Applications*, Prentice-Hall, New York (2001)
 - [28] Berendsen H. J. C., Grigera J. R. and T. P. Straatsma, *J. Phys. Chem.* **91**, 6269 (1987)
 - [29] Berendsen H. J. C., van der Spoel D., van Drunen R., *Comp. Phys. Comm.* **91**, 43 (1995)
 - [30] Hess B., Kutzner C., van der Spoel D. and Lindahl E., *J. Chem. Theory Comput.* **4**, 435 (2008)
 - [31] Van der Spoel D., Lindahl E., Hess B., Groenhof, G., Mark A. E. and Berendsen H. J. C., *J. Comp. Chem.* **26**, 1701 (2005)
 - [32] Oostenbrink C., Villa A., Mark A. E. and Van Gunsteren W. F. J. *Comp. Chem.* **25**, 1656 (2004)
 - [33] Weininger D., *J. Chem. Inf. Comput. Sci.* **28**, 31 (1988)
 - [34] <http://cactus.nci.nih.gov/services/translate/> (August 2010)
 - [35] Schüttelkopf A. W. and van Aalten D. M. F., *Acta Cryst.* **D60**, 1355 (2004)
 - [36] Ahlrichs R., Baer M., Haeser M., Hron M. and Koelmel C., *Chem. Phys. Lett.* **162**, 165 (1989)
 - [37] Weigend F., Haeser M., Patzelt H. and Ahlrichs R., *Chem. Phys. Lett.* **294**, 143 (1998)
 - [38] Haettig C., *Phys. Chem. Chem. Phys.* **7**, 59 (2005)
 - [39] Schaefer A., Klamt A., Sattel D., Lohrenz J. W. C. and Eckert F., *Phys. Chem. Chem. Phys.* **2**, 2187 (2000)
 - [40] Klamt A. and Schürmann G., *J. Chem. Soc. Perkin Trans.* **2**, 799 (1993)
 - [41] Essman U., Perela L., Berkowitz M. L., Darden T., Lee H. and Pedersen L. G., *J. Chem. Phys.* **103**, 8577 (1995)
 - [42] Hess B., Bekker H., Berendsen H. J. C. and Fraaije J. G. E. M., *J. Comp. Chem.* **18**, 1463 (1997)
 - [43] Beuler T. C., Mark A. E., van Schaik R. C., Gerber P. R. and van Gunsteren W. F., *Chem. Phys. Lett.* **222**, 529 (1994)
 - [44] McConlogue C. W. and Vanderlick T. K., *Langmuir* **13**, 7158 (1997)
 - [45] Milhiet P. E., Giocondi M.-C. and Le Grimmelc C., *Sci. World J.* **3**, 59 (2003)
 - [46] Benvegnu D. J. and McConnell H. M., *J. Phys. Chem.* **96**, 6820 (1992)
 - [47] May D., *Eur. Phys. J. E* **3**, 37 (2000)
 - [48] Ollila O. H. S., Risselada H. J., Louhivuori M., Lindahl E., Vattulainen I. and Marrink S. J., *Phys. Rev. Lett.* **102**, 0781011 (2009)
 - [49] Gaines G. L., *Insoluble Monolayers at Liquid-Gas Interfaces*, Wiley (Interscience), New York (1966)
 - [50] Baoukina S., Marrink S. J. and Tieleman D. P., *Faraday Discuss.* **144**, 393 (2010)
 - [51] Eisenhaber F., Lijnzaad P., Argos P., Sander C. and Scharf M., *J. Comp. Chem.* **16**, 273 (1995)
 - [52] Atkins P. W. and de Paula J., *Physical Chemistry*, Oxford University Press., Oxford 2006